Adaptive Resource Allocation for Energy-Efficient Millimeter-Wave Massive MIMO Networks

Sherif Adeshina Busari*, Kazi Mohammed Saidul Huq*, Ghassen Felfel* and Jonathan Rodriguez*,‡
*Instituto de Telecomunicações, 3810-193, Aveiro, Portugal
‡University of South Wales, Pontypridd, CF37 1DL, United Kingdom
Email: {sherifbusari, kazi.saidul, ghassenfelfel, jonathan}@av.it.pt; jonathan.rodriguez@southwales.ac.uk

***Abstract*—Massive, green, soft and super-fast are the key attributes that will describe next-generation mobile networks (5G and beyond). Large millimeter-wave (mmWave) bandwidths, massive MIMO antenna arrays, ultra-dense small cells (UDN) and cloud radio access network (C-RAN), among others, will enable these future networks to deliver huge performance gains. Since the networks are anticipated to be green and the available spectrum will be more abundant, energy efficiency (EE) becomes a more critical design factor than spectral efficiency (SE). In the face of competing potentials and challenges brought about by the different enablers, efficient resource allocation (RA) schemes are important to optimize system performance. In this work, we propose a fully-adaptive RA for a dense, C-RAN-enabled mmWave massive MIMO network. We then compare its performance to a non-adaptive and two semi-adaptive RA schemes. The fully-adaptive scheme outperforms all the other RA schemes and shows promising potentials for the joint EE-SE optimization of future mobile networks. Our results show the optimal EE-SE points and the impact of the transmit power and the number of data streams on the EE and SE performance.**

***Index Terms*—5G, C-RAN, energy efficiency, massive MIMO, mmWave, spectral efficiency.**

I. Introduction

The future mobile networks are envisaged to be massive. They will concurrently feature denser cells, larger bandwidths and a higher number of antennas than legacy cellular networks. Expectedly, they are anticipated to deliver huge performance gains across all fronts [1]. This ambitious target requires the massive networks to be green, soft and super-fast (i.e., energy-efficient, self-organizing and high-rate, respectively). These features will enable the networks to deliver optimal spectral efficiency (SE) and energy efficiency (EE) [2]. However, a joint optimization is very challenging, as a fundamental tradeoff typically exists between both metrics. More so, the large amount of network elements and radio resources involved makes such optimization even more tasking.

No doubt, the foreseen massive networks will deliver very high capacities. They will employ large millimeter-wave (mmWave) bandwidths and the large-scale antenna arrays (massive MIMO) to improve the networks' SE. This will lead to increased user throughputs in order to meet the skyrocketing traffic demands and improve the users' quality of experience (QoE) [1], [3]. On the other hand, the denser small cells (SCs) and the higher number of antennas in such networks intuitively imply higher overall power consumption. This trend therefore necessitates, more than ever before, the need for energy-efficient design schemes that will minimize the power consumption in order to lower the networks' energy utilization and carbon dioxide (CO_2) gas emission footprints [4].

More so, the energy consumption and gas emissions of communication networks are reaching alarming proportions, representing 2-3% of worldwide energy usage. The radio access networks (RANs) consume up to 70% of the total power of the network [2], [4]. These statistics are concerning, particularly from the perspectives of socio-economic and environmental concerns (i.e., costs, revenues, health, safety, environment, etc.). As a result, EE-SE co-design is a mandatory parameter for next-generation mobile networks (5G and beyond) to be viable and sustainable. It is, therefore, a critical component of 5G research [2].

For the overall improvement in system performance, all the radio resources (i.e., power, space, time and frequency) will have to be optimally utilized. Along this line, smart resource allocation (RA) schemes that optimize the power, spatial, temporal and spectral resources of the network have been proposed, largely for legacy networks. Newer, optimal RA schemes that consider the peculiar characteristics of propagation at mmWave frequencies in massive MIMO-enabled networks are, thus, subjects of active research. Among others, channel sparsity, near-line-of-sight (near-LOS) propagation, power and noise-limited operation are some of the features of mmWave massive MIMO that distinguish it from the rich-scattering, bandwidth-limited and interference-limited MIMO networks at microwave (μWave) frequencies [1]. Accordingly, the optimal 5G RA schemes aim to allocate the large bandwidth (BW) or time-frequency resource blocks (RBs) efficiently in the face of the power and noise limitations.

Many useful analyses and evaluations on optimal RA have been undertaken for varied scenarios and applications. In [5], the authors proposed an auction-based EE RA scheme for vehicular heterogeneous networks (HetNets). The EE RA schemes in [6] and [7] targeted device-to-device (D2D) communications, based on energy harvesting and cooperative relaying, respectively. Similar analysis has been done in [8] for heterogeneous cloud radio access networks (H-CRAN). These works provided efficient algorithms but did not consider mmWave massive MIMO. In [9], the authors proposed RA algorithms that maximize the proportional fairness (PF) spectral efficiency in mmWave massive MIMO. The work focused on SE and user fairness; it did not consider EE. User

association for joint SE-EE optimization was considered in [10]. The scenario, however, was for mmWave backhaul small cell (SC) networks.

In this work, we propose a novel fully-adaptive RA scheme that optimizes the joint EE-SE performance of a mmWave massive MIMO network. We compare the performance of the algorithm with a non-adaptive and two semi-adaptive schemes. Our system model features the partially/sub-connected hybrid precoding (HP) [11] architecture and CRAN-based scheduling. The simulations employ non-uniform cell load and user distribution, realistic mmWave channel model [12] and standard-compliant orthogonal frequency division multiplexing (OFDM) frame structure for 5G new radio (NR) [13]. To the authors' best knowledge, this investigation is the first to assess system-level performance using all the above-mentioned features collectively for joint SE-EE optimization.

The remainder of this paper is organized as follows. In Section II, we present the system model and describe the network layout, channel model, antenna configurations and the employed performance metrics. In Section III, we discuss the four RA schemes and provide their algorithms. Results and discussions follow in Section IV, while conclusion and the future research direction are presented in Section V.

II. System Model

This section describes the network model in terms of the deployment scenario, antenna and propagation models employed and the RA schemes investigated.

A. Network Deployment

We consider a single-cell architecture with a cluster of $J = 5$ mmWave SCs deployed in an area of $200 \times 200\, m^2$ in a downlink set-up. This represents a dense network as the inter-site distance (ISD) is typically less than 100 m. The clustered SCs are connected by wireless fronthaul to the C-RAN for RA. The centralized scheduler controls the power allocation and radio resource assignment for the cluster. All the SCs and the user equipment (UEs) are randomly deployed, as illustrated in the Voronoi diagram of Fig. 1. For each simulation, 1000 random simulation runs (nRuns) with 100 channel realizations or transmission time intervals (nTTIs) per run were undertaken. Thus, Fig. 1 is only a representative layout out of many random possibilities.

The random deployment leads to irregular cell sizes and varied user distributions as the SC-UE attachment is based on the highest signal-to-noise-ratio (SNR) criterion. The layout also affords the SCs with no load or attached users to go into sleep mode thereby bringing additional energy savings for the network. We consider an outdoor scenario with $(x_{SC}, y_{SC}, 10)\, m$ and $(x_{UE}, y_{UE}, 1.5)\, m$ and assume LOS environment. This assumption is valid as the transmission links are most likely to be in LOS conditions for the outdoor, dense, mmWave network considered [14].

B. mmWave Massive MIMO: Antenna and Channel Model

Massive arrays employing a dedicated radio frequency (RF) chain per antenna element (i.e., digital precoding (DP)) will greatly increase the power consumption, cost, computational complexity and signal processing demands of the network [11]. Analog beamforming (AB), on the other hand, can not provide the expected multiplexing gains. In response, HP which effectively reduces the required number of transceivers (or RF chains) without significant performance loss addresses this challenge [1], [11], [15].

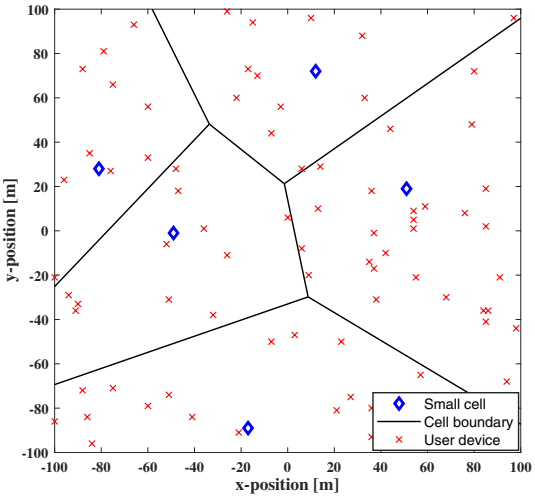

Fig. 1. Layout of Network Deployment

We, therefore, consider a massive MIMO model where each SC in the cluster is equipped with a uniform planar array (UPA) with $N \times M$ antenna elements along the y- and z-axis, respectively. For the HP considered, N represents the number of data streams (or employed RF chains N_{RF}) while M denotes the number of antenna elements (along the vertical or for each N_{RF}) used for beam steering. The array has $\lambda/2$ inter-element spacing both in the horizontal and vertical dimensions. On the other hand, single antenna elements are considered for the UEs, such that the total number of users in the network is $K = \sum_{SC=1}^{J} K_{SC}$.

The sub-connected HP architecture with N RF chains and NM phase shifters (PS) is employed. This is more energy-efficient and easier to implement for mmWave massive MIMO than the fully-connected HP architecture which requires N RF chains and N^2M PSs [11], [15]. The received signal vector $\mathbf{y} = [y_1, y_2, ..., y_K]^T$ at the users can be modeled as

$$\mathbf{y} = \sqrt{\rho}\mathbf{HADs} + \mathbf{n} = \sqrt{\rho}\mathbf{HPs} + \mathbf{n} \tag{1}$$

where ρ is the average received power, $\mathbf{H} \in \mathbb{C}^{\mathbf{K}\times\mathbf{NM}}$ denotes the channel matrix, $\mathbf{A} \in \mathbb{C}^{\mathbf{NM}\times\mathbf{K}}$ and $\mathbf{D} \in \mathbb{C}^{\mathbf{N}\times\mathbf{N}}$ are the analog and digital precoder matrices, respectively. $\mathbf{P}(= \mathbf{AD}) \in \mathbb{C}^{\mathbf{NM}\times\mathbf{N}}$ is the hybrid precoder matrix, while $\mathbf{s} \in \mathbb{C}^{\mathbf{K}\times\mathbf{1}}$ and $\mathbf{n} \in \mathbb{C}^{\mathbf{K}\times\mathbf{1}}$ are the user data and noise vectors, respectively.

The sum received power by a user k, $P_{r,t}^k$ is given as

$$P_{r,t}^k = P_{TX}^l \cdot G_{TX} \cdot G_{RX} \cdot PL \cdot SF \cdot |h_{r,t}|^2 \tag{2}$$

where P_{TX}^{l} is the transmit power on the particular layer/stream/TX-RX beam, G_{TX} is the transmitter gain, G_{RX} is the receiver gain, PL is the path loss, SF is the shadow fading loss and $h_{r,t}$ is the fast-fading [16].

The mmWave channel employed follows the implementation in [12]. It is a 3D statistical spatial channel model (SSCM) which uses the time cluster-spatial lobe (TCSL) approach. We consider a directional mmWave channel. The effective path loss (PL and SF) is

$$PL = 20\log_{10}\left(\frac{4\pi f}{c}\right) + 10\bar{n}\log_{10} d_{3D} + X_{\sigma} \tag{3}$$

where f is the carrier frequency, c is the speed of light, $\bar{n}$ is the path loss exponent (PLE), d_{3D} is the BS-UE separation distance and X_{σ} is the zero-mean log-normal random variable (SF) with standard deviation σ [17], [18].

For each transmission link, the channel impulse response (CIR) is generated for T time clusters (TCs) and S cluster subpaths (SPs). The directional channel h_{dir} for each TX-RX pair can be presented as

$$\begin{aligned} h_{dir}(t,\phi,\theta) = \sum_{t=1}^{T}\sum_{s=1}^{S_t} a_{s,t}e^{j\varphi_{s,t}} \cdot \delta(t-\tau_{s,t}) \\ \cdot g_{TX}(\phi-\phi_{s,t}) \cdot g_{RX}(\theta-\theta_{s,t}) \end{aligned} \tag{4}$$

where $a_{s,t}$, $\varphi_{s,t}$ and $\tau_{s,t}$ represent the magnitude, phase and propagation time delay of the s^{th} SP for the t^{th} TC, respectively. $\phi_{s,t}$ and $\theta_{s,t}$ are the azimuth (A) and elevation/ zenith (Z) angles, respectively. They both denote the departure angles at the BS (AoD, ZoD) and arrival angles at the UE (AoA, ZoA), respectively. The directive antenna gains g_{TX} and g_{RX} can be parameterized as

$$G(\phi,\theta) = \max\left(G_0 e^{\alpha\phi^2+\beta\theta^2}, \frac{G_0}{100}\right) \tag{5}$$

$$\alpha = \frac{4\ln(2)}{\phi_{3dB}^2}, \quad \beta = \frac{4\ln(2)}{\theta_{3dB}^2}, \quad G_0 = \frac{41253\xi}{\phi_{3dB}^2\theta_{3dB}^2} \tag{6}$$

where G_0 is the maximum directive boresight gain, α and β depends on ϕ_{3dB} and θ_{3dB} which are the azimuth and elevation half power beamwidths (HPBW), respectively, and ξ is the average antenna efficiency [17], [18].

The standard-compliant frame structure OFDM numerology for 5G/NR (mode 3) is employed. The maximum number of RBs (B) is 275 where a unit RB (W) is $1.44\,MHz$. Therefore, the maximum supported bandwidth $B \cdot W = 396\,MHz$ [13].

C. Performance Metrics

The cell throughput/sum data rate R is measured in "bits per second $[b/s]$". SE is the "throughput per unit spectrum $[(b/s)/Hz]$" while EE is evaluated in "bits per unit Joule $[b/J]$" [19]. Equations (7) and (8) establish R's relationship with SE and EE, respectively.

$$SE = \frac{Throughput\,(R)}{Bandwidth\,(B \cdot W)} \tag{7}$$

TABLE I
KEY SIMULATION PARAMETERS

Parameter	Value	Parameter	Value
f	28 GHz	BW [13]	396 MHz
$X(\mu,\sigma)$	(0,7) dB	B [13]	275 RBs
c	3×10^8	$\bar{n}$ [12]	2
N_o	-174 dBm/Hz	$\phi_{dB(SC)}$ [12]	10^o
NF	7 dB	$\theta_{dB(SC)}$ [12]	10^o
P_{TX}	[0-35] dBm	$\phi_{dB(UE)}$ [12]	10^o
K	[40, 80]	$\theta_{dB(UE)}$ [12]	10^o
NM	64	ξ [17]	0.7
N	[1-64]	P_{RF} [11]	250 mW
M	[64-1]	P_{PS} [11]	1 mW
$nRuns$	1000	L_{CD} [14]	100 $mW/(Gb/s)$
$nTTIs$	100	L_{BH} [14]	250 $mW/(Gb/s)$

$$EE = \frac{Throughput\,(R)}{Consumed\ Power\,(P_{total})} \tag{8}$$

For the considered network architecture, the throughput, R and the power consumption model, P_{total} can be modeled as:

$$R = \sum_{j=1}^{J}\sum_{k=1}^{K_j} B_{j,k}W \cdot \log_2\left(1 + \frac{P_{TX}^{k} \cdot h_{j,k}^{l}}{N_o \cdot B_{j,k}W \cdot NF}\right) \tag{9}$$

$$\begin{aligned} P_{total} = \overbrace{P_{TX}}^{\text{transmit}} + \overbrace{N \cdot P_{RF} + N \cdot M \cdot P_{PS}}^{\text{circuit (static)}} \\ + \underbrace{R\,(L_{CD} + L_{BH})}_{\text{circuit (dynamic)}} \end{aligned} \tag{10}$$

where N_o is the noise power spectral density, NF is the noise figure, P_{TX} is the transmitted/radiated power, P_{RF} and P_{PS} represent the power consumed by each RF chain and PS, respectively. The P_{PS} includes power consumed for excitation and insertion loss compensation [11]. R is the throughput; L_{CD} is the power consumed for coding per b/s and L_{BH} is the power used for backhauling per b/s [14]. The values for the key system parameters are presented in Table I.

III. Resource Allocation (RA) Schemes

Optimal RA scheme for dense networks requires a panoramic view of the load and traffic demands in the entire network for efficient scheduling. C-RAN enables self-organizing network (SON) which can adapt the RA for load balancing, interference mitigation, energy savings and overall network optimization. More so, SON will be mandatory in 5G, unlike in 4G systems where it is an optional feature. With the expected reduction in power consumption and centralized/dynamic RA, HP and C-RAN will enable the EE-SE joint optimization for the envisioned green, soft and super-fast, massive 5G networks.

We consider four RA schemes, as shown in Algorithm 1. The outputs from the algorithm are the powers, P_{TX}^{k} and the number of RBs, $B_{j,k}$ assigned to each user k. Scheme-I serves as the baseline where the RBs are homogeneously (i.e., almost-equally) assigned to the SCs irrespective of the SC load, and homogeneously allocated to the users irrespective

of their cell loads. In addition, equal layer power assignment is adopted regardless of the channel conditions. The semi-adaptive Scheme-II adapts the RB assignment based on the number of users attached to each SC. Per-layer power allocation is homogeneous (i.e., equal and independent of the channel).

For the semi-adaptive Scheme-III, per-layer power allocation is proportional to the channel gains but RB assignment per SC is homogeneous regardless of the cell load. Finally, we then propose the fully-adaptive Scheme-IV which adapts both the power and RB assignment. Here, per-layer or per-beam power to a user terminal is proportional to its channel strength and per-SC RB assignment is relative to the number of users attached to each cell. Unlike Scheme-I, the semi-adaptive and fully-adaptive schemes enable SCs to go into sleep mode when they have no attached users. This facilitates additional energy savings from the sleeping nodes.

IV. Simulation Results

In this section, we present the simulation results for the four RA schemes as described in Section III. With the emphatic interest on EE for sustainable future mobile networks, our evaluation seeks to identify the optimal P_{TX}, N_{RF} and EE-SE tradeoff points.

A. Optimal Transmit Power

The EE and SE performance with respect to the P_{TX} for the four RA schemes are shown in Fig. 2. For all cases, the results show that SE increases as P_{TX} increases for the considered power range. It is instructive to note that this trend is due to the fact that interference-free set-up is considered by employing precoding and disjoint RB assignment. There is no interference among the SCs within a cluster. Therefore, SINR reduces to SNR.

The EE performance has a different trend as also shown in Fig. 2. It first increases, peaks at the optimal P_{TX} and then continues to degrade thereafter. Two sets of points are noteworthy from the EE curves. The first set, for all RA schemes, appears at $P_{TX} = 20\,dBm$ for the considered scenario. This point gives the maximum EE, but reduced SE. The second set of points is where the EE and SE curves intersect (with P_{TX} between 25 and 27 dBm for all schemes). These points are the optimal points that jointly optimize both the EE and SE for the considered scenario.

With respect to the RA schemes, the fully-adaptive Scheme-IV outperforms all the others, as an adaptation to both channel conditions and cell load is enabled. Scheme-III has the worst performance. Homogeneous RBs corresponds to equal noise level (which is dependent on BW) in each channel. Adapting the power proportional to the channel gains enhances the good channels and degrades the performance of the weak channels. This leads to the overall reduction in the sum performance as compared to others. Comparison of the performance of schemes I-III show that RB adaptation is of more significance than power adaptation for the downlink while adaptation of both power and RB (Scheme-IV) gives the best result.

Algorithm 1: Resource Allocation (RA) Schemes

Inputs :

$\mathcal{J} = \{1, 2, ..., J\}$: *SCs*

$\mathcal{K}_{\mathcal{J}} = \{1, 2, ..., K_j\},\ \forall j \in \mathcal{J}$: *UEs per SC*

$K = \sum_{j=1}^{J} K_j$: *Total UEs (for all SCs)*

$B = \sum_{j=1}^{J} \sum_{k=1}^{K_j} B_{j,k}$: *Total RBs (for all SCs)*

$\mathcal{L} = \{1, 2, ..., L\}$: *Number of layer per SC*

$P_{TX} = \sum_{l=1}^{L} P_{TX}^{l}$: *TX power per SC*

$|h_{l,k}^{j}|$: *Channel gain (for each user k)*

Outputs:

P_{TX}^{k} : *Power allocation per user*

$B_{j,k}$: *RB allocation per user*

for $j \rightarrow 1$ **to** J **do**

$$\chi_{j,k}\left(\varsigma_n\right) = \begin{cases} 1, & \forall k \in \mathcal{L}\ (\forall n\ assigned\ to\ k) \\ 0, & otherwise \end{cases}$$

Scheme-I: Homogeneous P_{TX}^{k} and $B_{j,k}$

$B_j = Q = \frac{B}{J}; \qquad b_n = 0$

while $b_n < B_j \quad and \quad Q > 0$ **do**

  $b_n = b_n + 1; \qquad Q = Q - 1$

  $\texttt{Assign}\,(b_n \rightarrow K_{mod(Q,K_j)+1})$

for $k \rightarrow 1$ **to** K_j **do**

  $P_{TX}^{k} = \chi_{j,k} \frac{P_{TX}}{L}$

  $B_{j,k} = \varsigma_n \sum_{n=1}^{B_j} b_n$

Scheme-II: Homogeneous P_{TX}^{k}, Adaptive $B_{j,k}$

$B_j = \frac{K_j}{K} \times B$

for $k \rightarrow 1$ **to** K_j **do**

  $P_{TX}^{k} = \chi_{j,k} \frac{P_{TX}}{L}$

  $B_{j,k} = \frac{|h_{l,k}^{j}|}{\sum_{k=1}^{K_j} |h_{l,k}^{j}|} \times B_j$

Scheme-III: Adaptive P_{TX}^{k}, Homogeneous $B_{j,k}$

$B_j = Q = \frac{B}{J}; \qquad b_n = 0$

while $b_n < B_j \quad and \quad Q > 0$ **do**

  $b_n = b_n + 1; \qquad Q = Q - 1$

  $\texttt{Assign}\,(b_n \rightarrow K_{mod(Q,K_j)+1})$

for $k \rightarrow 1$ **to** K_j **do**

  $P_{TX}^{k} = P_{TX} \cdot \frac{|h_{l,k}^{j}|}{\sum_{k=1}^{K_j} |h_{l,k}^{j}|} \cdot h_k$

  $B_{j,k} = \varsigma_n \sum_{n=1}^{B_j} b_n$

Scheme-IV: Adaptive P_{TX}^{k} and $B_{j,k}$

$B_j = \frac{K_j}{K} \times B$

for $k \rightarrow 1$ **to** K_j **do**

  $P_{TX}^{k} = P_{TX} \cdot \frac{|h_{l,k}^{j}|}{\sum_{k=1}^{K_j} |h_{l,k}^{j}|} \cdot h_k$

  $B_{j,k} = \frac{|h_{l,k}^{j}|}{\sum_{k=1}^{K_j} |h_{l,k}^{j}|} \times B_j$

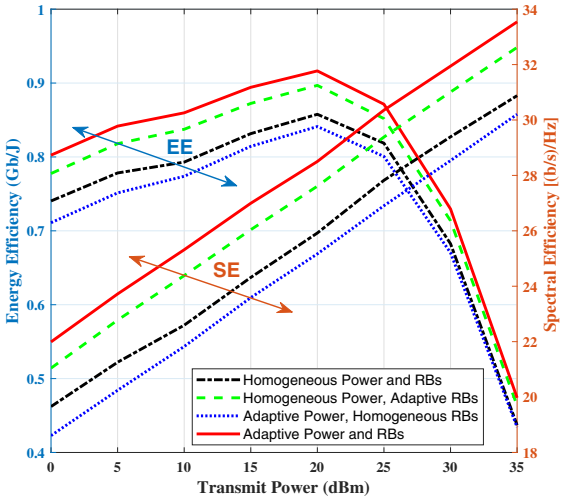

Fig. 2. EE-SE performance as a function of P_{TX}

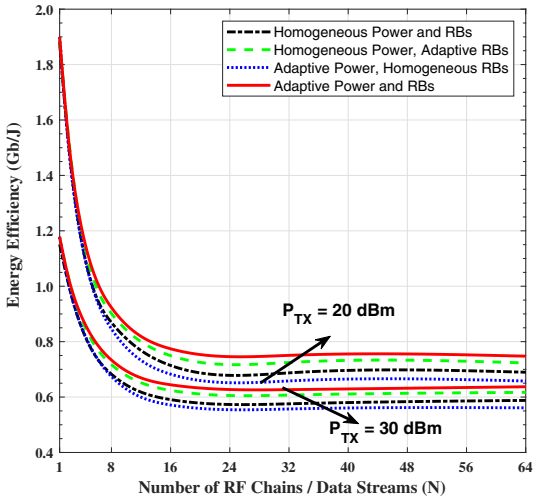

Fig. 3. EE vs N_{RF} performance $[K = 8]$

B. Sufficient Number of RF Chains/Data Streams

In terms of power consumption, AB and DP represent the two extreme cases. AB consumes the least power for single stream transmission. DP, on the other hand, consumes the most by employing RF chains/data streams equal to the number of antenna elements. For massive MIMO arrays, HP offers a significant reduction in the number of required RF chains and the associated energy consumption and cost (when compared with DP), yet achieving near-optimal performance.

Fig. 3 shows the EE performance as a function of the required number of RF chains or data streams (N). For each SC, $NM = 64$, $N = [1, ..., 64]$ and $K = 8$ on the average. Two sets of plots are shown: $P_{TX} = 20\,dBm$ and $P_{TX} = 30\,dBm$. The trend in both sets are similar. However, the plot for $P_{TX} = 20\,dBm$ has EE performance gain of 0.1 Gb/J for all RA schemes considered. Recall that, in Fig. 2 of subsection IV-A, $P_{TX} = 20\,dBm$ is the optimal transmit power for the considered network, hence the performance gain over the plots for $P_{TX} = 30\,dBm$ which is suboptimal for the scenario under consideration.

In addition, Fig. 3 also shows that the EE performance saturates from around $N = 16$ for both power sets and all RA schemes. For the set-up, $K = 8$ in each cell, on average. This shows that RF chains equal to twice the number of served antennas per cell (i.e., $N = 2K$) is sufficient for optimal operation as the EE saturates beyond this point. Additional data streams do not bring any benefit in terms of EE.

Similarly, Fig. 4 shows the EE performance as a function of N_{RF} for $K = 8$ and $K = 16$. For both cases, $P_{TX} = 30\,dBm$. The plots again buttress the deduction that $N = 2K$ is sufficient for optimal operation. The EE performance saturation begins at $N = 16$ when $K = 8$, and at $N = 32$ when $K = 16$.

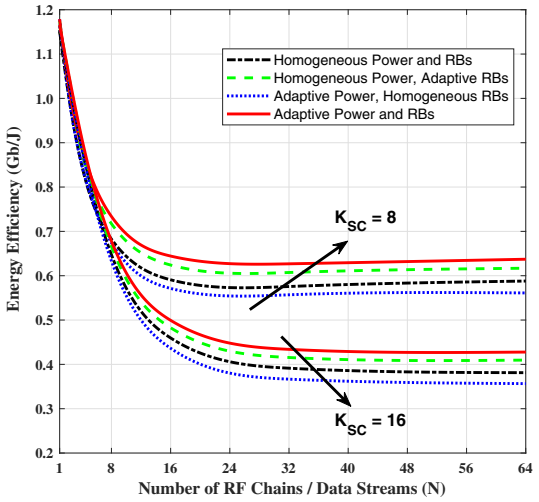

Fig. 4. EE vs N_{RF} performance $[P_{TX} = 30\,dBm]$

C. EE-SE Performance Tradeoff

Fig. 5 shows the EE-SE performance curve for the considered network. For each RA scheme, the curve shows that EE first starts to increase as SE increases. It then reaches the optimal point. Beyond this point, the EE begins to degrade though the SE continues to increase. For green mmWave massive MIMO systems where EE is a critical factor, it is desirable not to operate beyond the optimal EE point. As shown in Fig. 5, Scheme-IV again outperforms all the other schemes for the same reasons explained in subsection IV-A. It achieves both higher EE and SE at the optimal points than the other schemes due to the full adaptation of RB assignment to the cell load and the full adaptation of power to the channel conditions.

The EE-SE performance curve is shown in Fig. 5. The trend

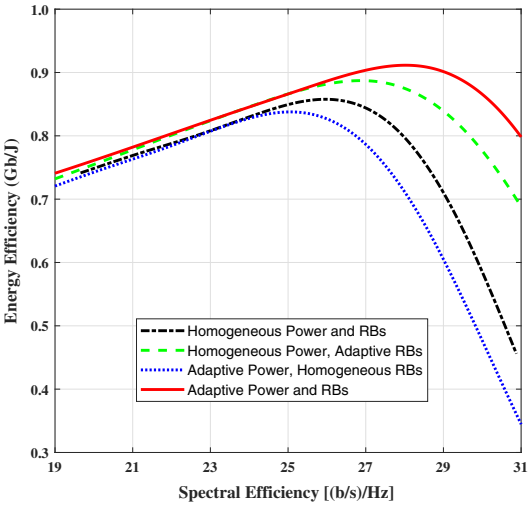

Fig. 5. EE vs SE performance tradeoff curve

is consistent with results in [2], [4], [15], [19]. On the quasi-concave nature of the curves, [19] established that the trend is due to the impact of the static circuit power. Recall that the power model in (10) consists of the transmit power, the dynamic circuit power (that scales with the throughput) and the static circuit power (which is independent of the data rate, SE and BW of the network). The static power plays a pivotal role in shaping the EE-SE tradeoff relationship. Finding the optimal EE and SE is fundamental to realizing green 5G networks.

V. Conclusion and Future Work

In this paper, we have demonstrated that a fully-adaptive RA scheme provides better EE performance than semi-adaptive and non-adaptive RA schemes. We have also shown that data streams or RF chains equal to twice the number of receive antennas are sufficient for energy-efficient mmWave massive MIMO network. This realization reduces the number of required RF chains and, correspondingly, the power consumption in the system. A fully-adaptive RA, therefore, provides the framework to dynamically turn on the required number of streams/layers. This can bring additional energy savings and overall improvement in EE, as amply shown in the results. Using the EE-SE performance curve, our results also reveal the optimal operating point of the system desirable for the operation of green mobile networks of the future. Extension of this work to multi-cell scenarios is the direction for future work.

Acknowledgment

Sherif Busari and Kazi Huq would like to acknowledge their PhD and Post-doc grants funded by the Fundação para a Ciência e a Tecnologia (FCT-Portugal) with reference nos. PD/BD/113823/2015 and SFRH/BPD/110104/2015, respectively. Also, the research leading to these results received funding from the European Commission H2020 program under grant agreement no. 815178 (5GENESIS project).

References

[1] S. A. Busari, K. M. S. Huq, S. Mumtaz, L. Dai, and J. Rodriguez, "Millimeter-Wave Massive MIMO Communication for Future Wireless Systems: A Survey," *IEEE Communications Surveys & Tutorials*, vol. 20, no. 2, pp. 836–869, Secondquarter 2018.

[2] C.-L. I, "Seven fundamental rethinking for next-generation wireless communications," *APSIPA Transactions on Signal and Information Processing*, vol. 6, p. e10, 2017.

[3] S. A. Busari, S. Mumtaz, S. Al-Rubaye, and J. Rodriguez, "5G Millimeter-Wave Mobile Broadband: Performance and Challenges," *IEEE Communications Magazine*, vol. 56, no. 6, pp. 137–143, June 2018.

[4] K. M. S. Huq, S. Mumtaz, J. Bachmatiuk, J. Rodriguez, X. Wang, and R. L. Aguiar, "Green HetNet CoMP: Energy Efficiency Analysis and Optimization," *IEEE Transactions on Vehicular Technology*, vol. 64, no. 10, pp. 4670–4683, Oct 2015.

[5] Z. Zhou, F. Xiong, C. Xu, Y. He, and S. Mumtaz, "Energy-Efficient Vehicular Heterogeneous Networks for Green Cities," *IEEE Transactions on Industrial Informatics*, vol. 14, no. 4, pp. 1522–1531, April 2018.

[6] Z. Zhou, C. Gao, C. Xu, T. Chen, D. Zhang, and S. Mumtaz, "Energy-Efficient Stable Matching for Resource Allocation in Energy Harvesting-Based Device-to-Device Communications," *IEEE Access*, vol. 5, pp. 15 184–15 196, 2017.

[7] C. Xu, J. Feng, Z. Zhou, Z. Chang, Z. Han, and S. Mumtaz, "Two-Stage Matching for Energy-Efficient Resource Management in D2D Cooperative Relay Communications," in *GLOBECOM 2017 - 2017 IEEE Global Communications Conference*, Dec 2017, pp. 1–6.

[8] M. Peng, K. Zhang, J. Jiang, J. Wang, and W. Wang, "Energy-Efficient Resource Assignment and Power Allocation in Heterogeneous Cloud Radio Access Networks," *IEEE Transactions on Vehicular Technology*, vol. 64, no. 11, pp. 5275–5287, Nov 2015.

[9] I. Ahmed, H. Khammari, and A. Shahid, "Resource Allocation for Transmit Hybrid Beamforming in Decoupled Millimeter Wave Multiuser-MIMO Downlink," *IEEE Access*, vol. 5, pp. 170–182, 2017.

[10] A. Mesodiakaki, F. Adelantado, L. Alonso, M. D. Renzo, and C. Verikoukis, "Energy- and Spectrum-Efficient User Association in Millimeter-Wave Backhaul Small-Cell Networks," *IEEE Transactions on Vehicular Technology*, vol. 66, no. 2, pp. 1810–1821, Feb 2017.

[11] X. Gao, L. Dai, S. Han, C. L. I, and R. W. Heath, "Energy-Efficient Hybrid Analog and Digital Precoding for MmWave MIMO Systems With Large Antenna Arrays," *IEEE Journal on Selected Areas in Communications*, vol. 34, no. 4, pp. 998–1009, April 2016.

[12] New York University. (2017) NYUSIM v1.6. [retrieved: 2018-04-26]. [Online]. Available: http://wireless.engineering.nyu.edu/5g-millimeter-wave-channel-modeling-software/

[13] 3GPP. (2018) TS 38.211 Technical Specification Group Radio Access Network; NR, Physical channels and modulation v15.1.0. [retrieved: 2018-04-26]. [Online]. Available: http://www.3gpp.org/ftp//Specs/archive/38_series/38.211/

[14] A. Pizzo and L. Sanguinetti, "Optimal design of energy-efficient millimeter wave hybrid transceivers for wireless backhaul," in *2017 15th International Symposium on Modeling and Optimization in Mobile, Ad Hoc, and Wireless Networks (WiOpt)*, May 2017, pp. 1–8.

[15] S. Han, C. l. I, Z. Xu, and C. Rowell, "Large-scale antenna systems with hybrid analog and digital beamforming for millimeter wave 5G," *IEEE Communications Magazine*, vol. 53, no. 1, pp. 186–194, Jan. 2015.

[16] S. A. Busari, S. Mumtaz, K. M. S. Huq, J. Rodriguez, and H. Gacanin, "System-Level Performance Evaluation for 5G mmWave Cellular Network," in *GLOBECOM 2017 - 2017 IEEE Global Communications Conference*, Dec 2017, pp. 1–7.

[17] M. K. Samimi and T. S. Rappaport, "3-D Millimeter-Wave Statistical Channel Model for 5G Wireless System Design," *IEEE Transactions on Microwave Theory and Techniques*, vol. 64, no. 7, pp. 2207–2225, July 2016.

[18] S. Sun, G. R. MacCartney, and T. S. Rappaport, "A novel millimeter-wave channel simulator and applications for 5G wireless communications," in *2017 IEEE International Conference on Communications (ICC)*, May 2017, pp. 1–7.

[19] K. M. S. Huq, S. Mumtaz, J. Rodriguez, and R. Aguiar, "Overview of Spectral- and Energy-Efficiency Trade-off in OFDMA Wireless System," in *Green Communication for 4G Wireless Systems*, S. Mumtaz and J. Rodriguez, Eds. River Publishers, Aalborg, 2013.